

Supplementary Materials to:

β -Lactoglobulin Adsorption Layers at the Water/Air Surface: 4. Impact on the Stability of Foam Films and Foams

Georgi G. Gochev ^{1,2,*}, Vamseekrishna Ulaganathan ³, Inga Retzlaff ⁴, Cécile Gehin-Delval ⁵, Deniz Z. Gunes ⁵, Martin Leser ⁵, Ulrich Kulozik ⁶, Reinhard Miller ^{4,7} and Björn Braunschweig ⁸

¹ Jerzy Haber Institute of Catalysis and Surface Chemistry, Polish Academy of Sciences, 30239 Krakow, Poland

² Institute of Physical Chemistry, Bulgarian Academy of Sciences, 1113 Sofia, Bulgaria

³ Institute of Biomaterial Science, Helmholtz-Zentrum Geesthacht, 14513 Teltow-Seehof, Germany; vamseekrishna.ulaganathan@hzg.de

⁴ Max Planck Institute of Colloids and Interfaces, 14476 Potsdam, Germany; inga.retzlaff@gmail.com

⁵ Nestlé Research Center, CH-1000 Lausanne 26, Switzerland; Cecile.Gehin-Delval@rdor.nestle.com (C.C.-D.), ZeynelDeniz.Gunes@rdls.nestle.com (D.Z.G.); Martin.Leser@rdls.nestle.com (M.L.)

⁶ Chair of Food and Bioprocess Engineering, TU Munich, 85354 Freising, Germany; ulrich.kulozik@tum.de

⁷ Department of Physics, TU Darmstadt, 64289 Darmstadt, Germany; miller@fkp.tu-darmstadt.de

⁸ Institute of Physical Chemistry and Center for Soft Nanoscience, WWU Münster, 48149 Münster, Germany; braunschweig@uni-muenster.de

* Correspondence: ncgochev@cyf-kr.edu.pl or gochev@ipc.bas.bg

Zeta potential data from literature

Figure S1 presents the pH dependences of the average number of protons bound to the protein Z_{H^+} obtained from hydrogen ion titration experiments [1] and the electrophoretic zeta potential ζ [2,3]. The data show that the isoelectric point (pI) is located within the pH range 4.9–5.3. Although both dependences exhibit similar shape, the ζ -values tend to level off earlier when moving away from pI . Note, in electrokinetic experiments the electric potential is probed at the shear plane while with hydrogen ion titration the number of titratable charged groups (thus the protein net charge) is directly obtained. However, it is not the purpose of this work to analyze these issues but just to illustrate the trend of the pH-dependent net charge of BLG in order to support the interpretation of other results based on charge-induced effects.

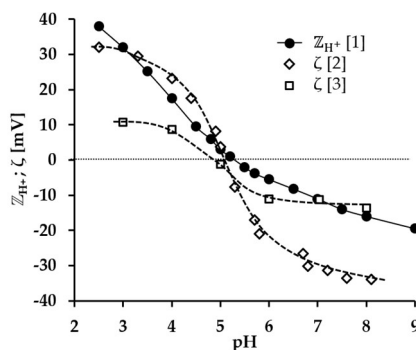


Figure S1. Average number of bound protons Z_{H^+} (adapted from [1]) and zeta potential ζ (adapted from Refs. [2,3]) for BLG solutions as a function of pH; (\diamond) pH adjusted by HCl/NaOH, (\square) McIlvaine buffer (10 mM citric acid + 20 mM Na_2HPO_4).

Foams

Figure S2 presents a ΔH_F vs. ΔH_L plot for a selected exemplary foam. It is seen in the inset at the right-hand side of the figure that the resolution of the measured heights is better than 0.5 mm. These data illustrate one of the ways (discussed in the main text) to estimate the value of t_{dev} .

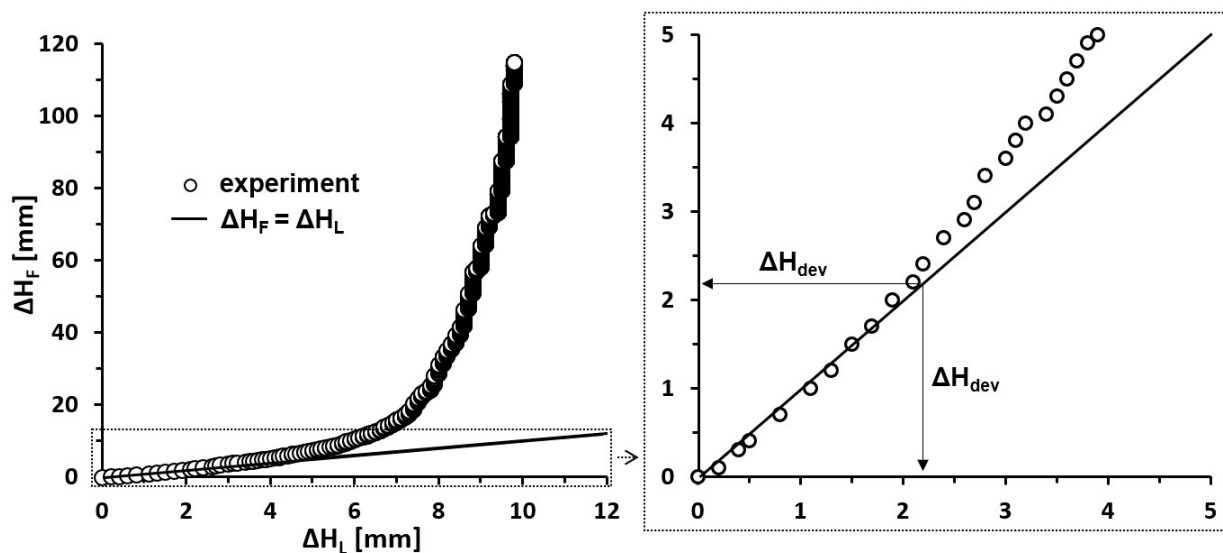


Figure S2. (left) ΔH_F vs. ΔH_L plot for foam obtained from 100 μM BLG solution at pH 3 and $C_{\text{buff}} = 10$ mM; a linear regression $\Delta H_F = \Delta H_L$ is shown for comparison. (right) Zoomed-in fragment of the main graph; the common value of ΔH_{dev} is that measured at t_{dev} .

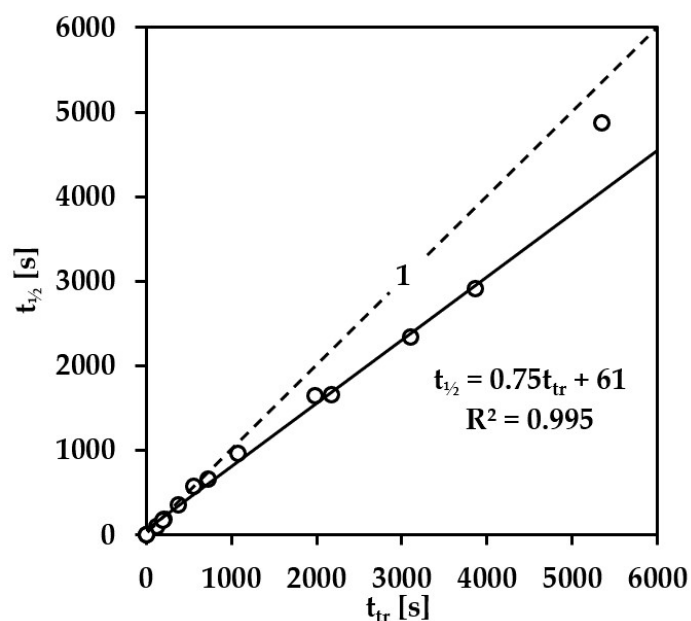


Figure S3. $t_{1/2}$ vs t_{tr} plot of the data in Figs. 8(b) and 9(b) in the main text. The solid line is a linear regression of the experimental data; the last data point at the longest times is omitted in the fitting.

It has been found earlier for surfactant foams that there is a linear relation between $t_{1/2}$ and t_{tr} [4] and this is also the case with our results on BLG foams. Fig. 10 presents a $t_{1/2}$ vs. t_{tr} plot constructed from the data in Figs. 8(b) and 9(b) in the main text. The $t_{1/2}(t_{\text{tr}})$ dependence follows a linear profile with a slope of 0.75, but interestingly, the values for $t_{1/2}$ and t_{tr} are very close for times up to about 1000 s. At the moment we do not have a convincing explanation for this relation, however, to tackle this issue more experiments for richer statistics would be needed.

Values of ΔH_{dev} and t_{dev} can be used to calculate the rate v_{dev} of liquid efflux in the initial stage of foam decay (t_0-t_{dev}):

$$v_{\text{dev}} = \Delta H_{\text{dev}}/t_{\text{dev}} \quad (\text{S1})$$

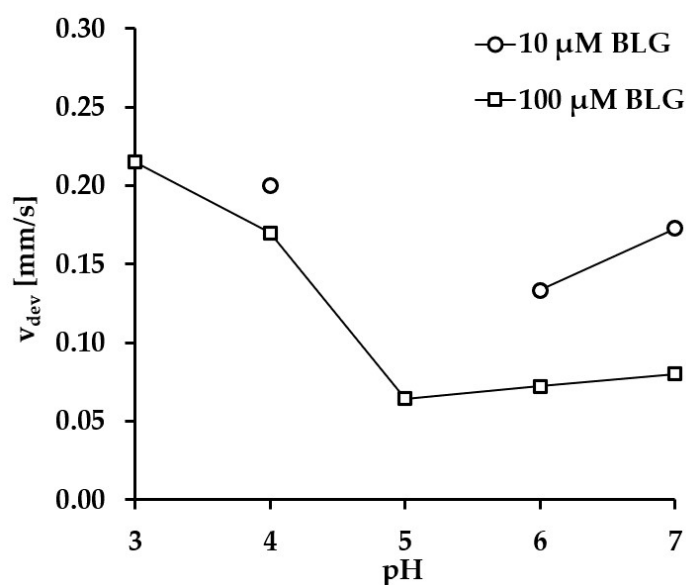


Figure S4. v_{dev} as a function of pH for two BLG concentrations.

On the basis of published data for the Sauter mean bubble radius r_{32} in fresh foams obtained in BLG solutions at different protein concentrations and pH [2,3,5] we could approximately estimate the capillary pressures $P_{c,F}$ in the studied foams via the relation $P_{c,F} = 2\gamma/r_{32}$. Since the surface tensions γ at the foam bubbles' surfaces are unknown, we introduce boundary conditions: 1) as a maximum surface tension we use $\gamma = 66$ mN/m, which was found to be the surface tension required to overcome instantaneous coalescence of two bubbles in BLG solutions [6]; 2) as a minimum surface tension we use $\gamma = 50$ mN/m, which approaches the lowest values measured in the surface tension isotherms for BLG solutions (pH 5, $C_{\text{buff}} = 10$ mM) [7]. Foams with average bubble sizes in the range between $r_{32} \approx 600$ μm and $r_{32} \approx 80$ μm have been reported for solutions with various C_{BLG} and pH obtained under the conditions of: frit pore size ~ 27 μm and gas flow rate of 400 ml/min [3]; or frit pore size $\sim 9\text{--}16$ μm and gas flow rate of 60 ml/min [2,5]. Hence, we obtained a spectrum of estimated capillary pressures spanning between a minimum of $P_{c,F}^{\text{min}} \approx 170$ Pa ($r_{32} \approx 600$ μm and $\gamma = 50$ mN/m) and a maximum of $P_{c,F}^{\text{max}} \approx 1.7$ kPa ($r_{32} \approx 100$ μm and $\gamma = 66$ mN/m) for all studied foams at C_{BLG} of 10 μM and 100 μM at any pH.

Thin foam films

Thin foam films were studied with a Scheludko-Exerowa tube cell (Fig. S5). A detailed description of the method is given elsewhere [8-10]. In brief, microscopic foam films (radius $r_f = 100$ μm) were obtained at constant capillary pressure P_c in a glass tube holder with a radius of $R = 1$ mm. A drop of the solution was situated in the film holder (glass tube) and left to rest 10 min before the formation of a film by sucking liquid from the solution drop through a capillary. The disjoining pressure Π of an equilibrium film equals to the capillary pressure P_c in the meniscus, which is estimated via the approximation $P_c \approx 2\gamma/R$, where γ is the surface tension of the solution. Since γ decreases with the increase of the protein concentration, in the present experiments P_c was found to vary between 140 and 100 Pa (for 0.1 μM and 10 μM BLG, respectively) according to the surface tension values of the same solutions measured after 10 min of adsorption [7].

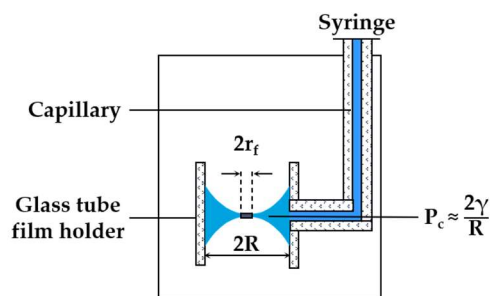


Figure S5. Schematic drawing of the Scheludko-Exerowa tube cell (r_f is film radius).

A freshly formed film was left to drain until rupture. In these experiments we investigated the probability $W_{bs} = N_{bs}/N$ (N_{bs} – number of films with black spot out of the total number of monitored films N) of formation of black spots in foam films obtained from solutions with pH 5 (in 10 mM buffer) at BLG concentrations in the range 0.1–10 μM . For each BLG concentration, values for $W_{bs} \times 100$ [%] were obtained by direct visual observations (note the reaction time of human eye is about 0.5 s) of 50 films and the results are presented in Fig. S6. At 0.1 μM black spots were not observed at all until film rupture, while at 1 μM every film ruptured through the formation of black spots. A stabilization of the NBF structure occurs at protein concentrations in the range $10 \mu\text{M} < C_{\text{BLG}} < 30 \mu\text{M}$ (a and b* in Fig. S6). A critical surfactant concentration – denoted by C_e as the equilibrium concentration for the formation of a stable NBF – has been earlier introduced for foam and emulsion NBFs from low-molecular-weight surfactant solutions as studied in a tube cell at relatively low disjoining pressures (usually below 140 Pa) [7,9]. Other characteristic concentrations introduced for surfactant films are the minimum surfactant concentration required for the formation of black spots in the films, denoted by C_{bl} , and the concentration at which always black films are obtained, denoted by C_t [9].

In summary, we found the characteristic concentrations of BLG for the formation and stability of foam NBFs under the studied solvent conditions (pH 5, $C_{\text{buff}} = 10 \text{ mM}$): $0.1 \mu\text{M} < C_{bl} < 0.2 \mu\text{M}$, $C_t = 1 \mu\text{M}$, $10 \mu\text{M} < C_e < 30 \mu\text{M}$.

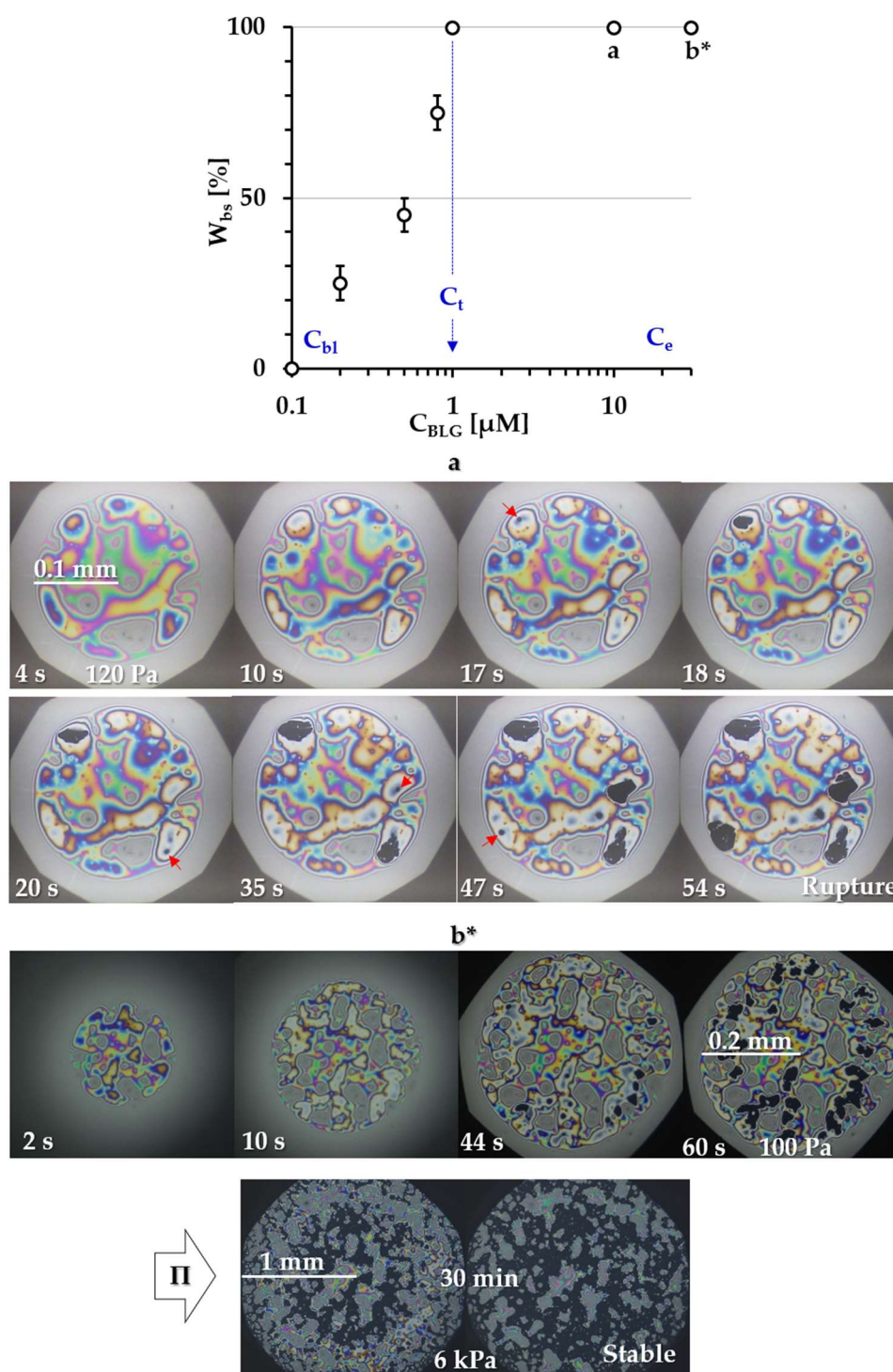


Figure S6. Effect of C_{BLG} (pH 5, $C_{buff} = 10$ mM) on the formation and stability of foam NBFs. W_{bs} is the probability for the observation of black spots in films obtained in a tube cell at capillary pressures of 120–140 Pa. C_{bl} , C_t and C_e are characteristic concentrations for the formation and stability of NBFs (see details in the text). **a.** ‘Unstable’ film at 10 μM BLG, arrows indicate the appearance of black spots. **b*.** Film at 30 μM BLG obtained in a porous plate cell at $\Pi = 100$ Pa; the last two photos show the same film at a disjoining pressure of $\Pi = 6$ kPa.

Tensiometry and dilational rheometry

Adsorption kinetics (0.1–80 s) was investigated by measurements of the dynamic surface pressure $\pi(t)$ ($\pi = \gamma_0 - \gamma$, where γ and $\gamma_0 = 72.3 \pm 0.2$ mN/m are the surface tensions of solution and pure buffer, respectively) at the surface of a growing air bubble at the tip of a steel capillary (radius

of 130 μm) immersed downward in a solution using the Maximum Bubble Pressure Tensiometer BPA-1S, Sinterface, Germany. More details about the technique are given elsewhere [11]. The measurements for each solution were performed at least in duplicates.

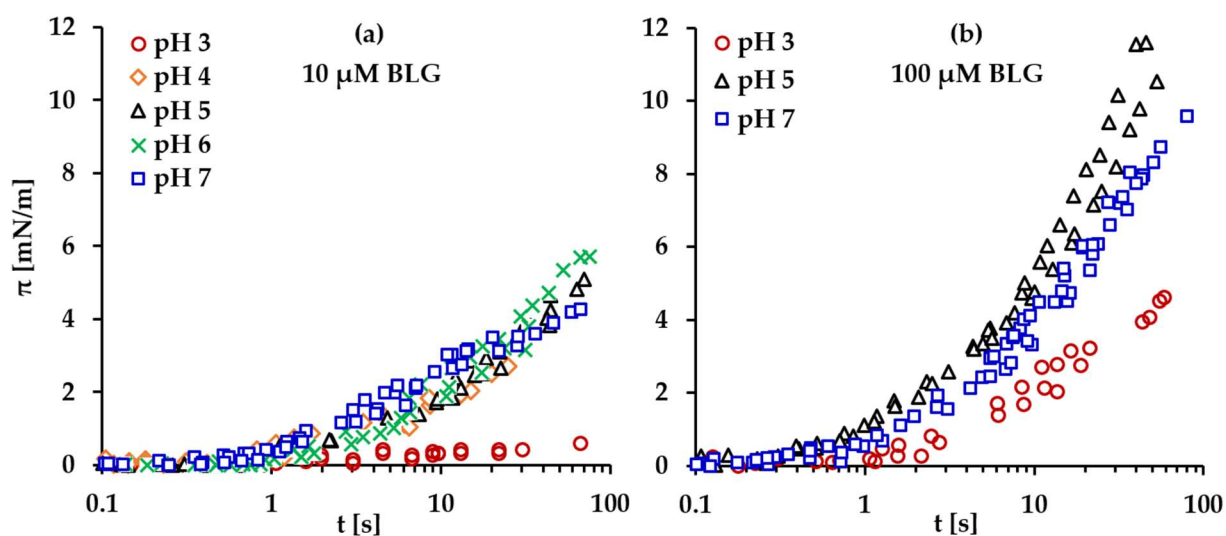


Figure S7. Dynamic surface pressure $\pi(t)$ for BLG adsorption at the surface of a growing air bubble as measured by Bubble Pressure tensiometry.

We studied the adsorption kinetics of BLG at the surface of a growing air bubble in BLG solutions at various pH values ($C_{\text{buff}} = 10 \text{ mM}$) in the time range 0.1–80 s. Fig. S7 presents dynamic surface pressure $\pi(t)$ data for both BLG concentrations used in this study. For $C_{\text{BLG}} = 10 \mu\text{M}$, the measurements revealed induction times τ_{ind} of $\sim 1 \text{ s}$ for any of the studied solutions at different pH, except for pH 3 where τ_{ind} was two orders of magnitude longer as shown in [7]. The parameter τ_{ind} is the time period where no change of the surface tension is detectable and induction times are frequently observed in the course of protein adsorption [7]. At longer adsorption times, up to 80 s, π increased to about 4–5 mN/m and virtually no effects of pH (4, 5, 6.3 and 7) were detected. For $C_{\text{BLG}} = 100 \mu\text{M}$, BLG solutions at pH 3, 5 and 7 were investigated and the measurements revealed decrease of τ_{ind} to the ms range for pH 5 and pH 7, and to about 2 s for pH 3. The lowest surface activity of BLG at pH 3 can be attributed to the largest protein net charge within the studied pH range [7] (see the titration data in Fig. S1(a)).

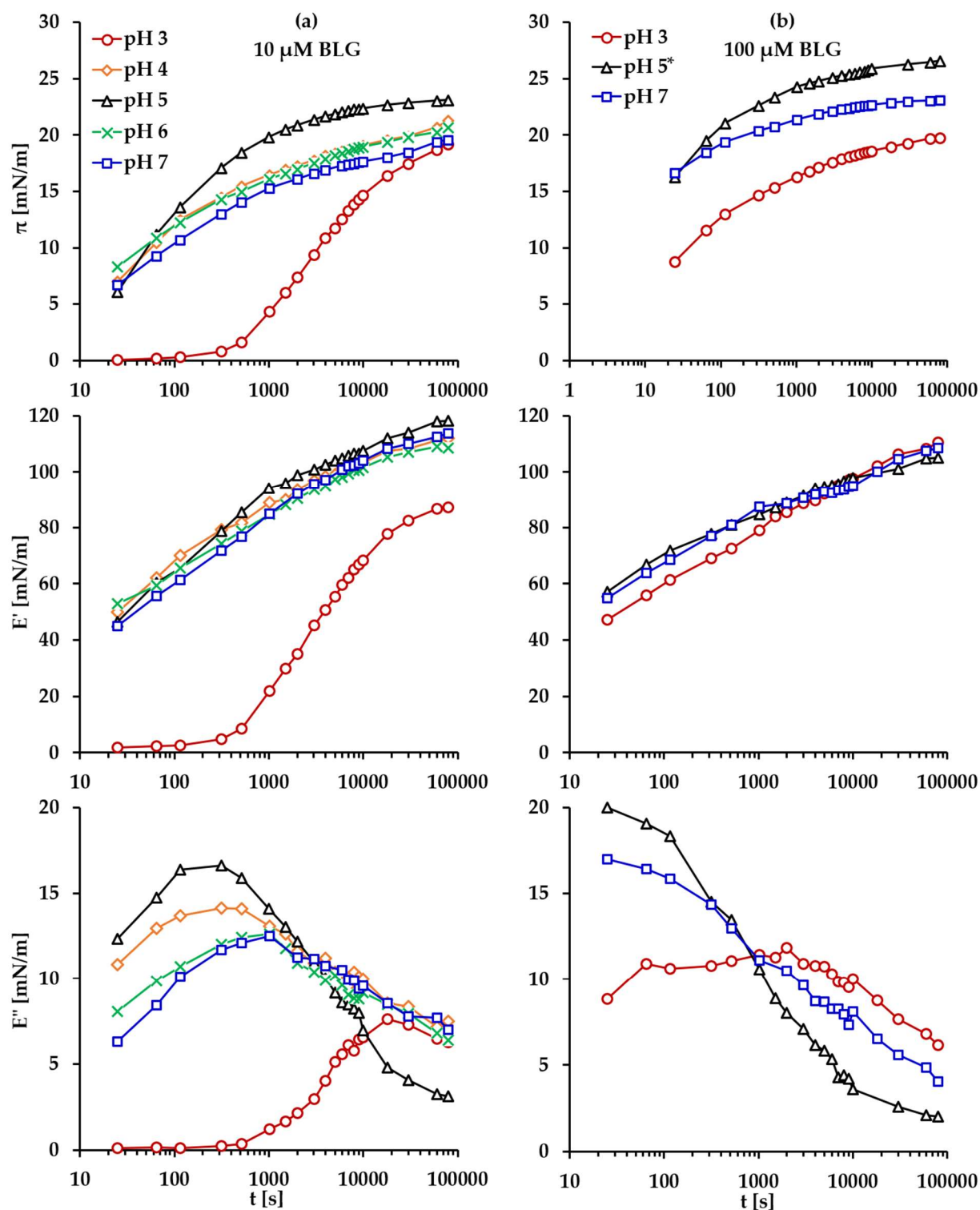


Figure S8. Kinetic dependencies of the surface pressure $\pi(t)$ and the elastic $E'(t)$ and viscous $E''(t)$ parts of the dilational viscoelastic modulus for BLG adsorption layers at the surface of a static air bubble as measured by Profile Analysis Tensiometry; taken from the data sets reported in [7,12]. * pH 5, $C_{\text{BLG}} = 20 \mu\text{M}$.

Dynamic surface pressure $\pi(t)$ was measured in long-time adsorption experiments for a buoyant bubble of volume $10 \mu\text{l}$ in solution by the Profile Analysis Tensiometer PAT-1M, Sinterface, Germany. To access values for the dilational rheology parameters, the bubble was periodically subjected to short sets of sinusoidal area oscillations at a frequency of 0.1 Hz and an area deformation of 7 %. Both the real E' (elastic contribution) and the imaginary E'' (viscous contribution) parts of the complex

viscoelasticity modulus were calculated from the surface tension response to the area oscillations and were monitored in the course of adsorption, thus obtaining the kinetic dependencies $E'(t)$ and $E''(t)$. Data from previous measurements [7,12] of BLG solutions at two protein concentrations of 10 μM and 100 μM , and at various pH values ($C_{\text{buff}} = 10 \text{ mM}$) are presented in Fig. S7.

References

- 1 S.K. Ghosh, S. Chaudhuri, J. Roy, N.K. Sinha, A. Sen. Physicochemical investigations on buffalo β -lactoglobulin. Studies on sedimentation, diffusion, and hydrogen ion titration. *Arch. Biochem. Biophys.* 144 (1971) 6-15.
- 2 K. Engelhardt, M. Lexis, G. Gochev, C. Konnerth, R. Miller, N. Willenbacher, W. Peukert, B. Braunschweig. pH effects on the molecular structure of β -lactoglobulin modified air-water interfaces and its impact on foam rheology. *Langmuir* 29 (2013) 11646-11655.
- 3 ^a F.J. Lech, Foam properties of proteins, low molecular weight surfactants and their complexes. PhD Thesis, Wageningen University, Wageningen, 2016; ^b F.J. Lech, R.J.B.M. Delahaije, M.B.J. Meinders, H. Gruppen, P.A. Wierenga. Identification of critical concentrations determining foam ability and stability of β -lactoglobulin. *Food Hydrocolloids* 57 (2016) 46-54.
- 4 K. Lunkenheimer, K. Malysa, K. Winsel, K. Geggel, S. Siegel. Novel Method and Parameters for Testing and Characterization of Foam Stability. *Langmuir* 26 (2009) 3883-3888.
- 5 M. Lexis, N. Willenbacher. Relating foam and interfacial rheological properties of β -lactoglobulin solutions. *Soft Matter* 10 (2014) 9626-9636.
- 6 J. Won, J. Krägel, G. Gochev, V. Ulaganathan, A. Javadi, A. Makievski, R. Miller. Bubble-bubble interaction in aqueous β -Lactoglobulin solutions. *Food Hydrocolloids* 34 (2014) 15-21.
- 7 V. Ulaganathan, I. Retzlaff, J. Won, G. Gochev, C. Gehin-Delval, M. Leser, B. Noskov, R. Miller. β -Lactoglobulin adsorption layers at the water/air surface: 1. Adsorption kinetics and surface pressure isotherm: effect of pH and ionic strength. *Colloids Surfaces A* 519 (2017) 153-160.
- 8 D. Platikanov, D. Exerowa. *Fundamentals of Foam Films*. in: D. Exerowa, G. Gochev, D. Platikanov, L. Liggieri, R. Miller (Ed.) *Foam Films and Foams: Fundamentals and Applications*. CRC Press, Boca Raton, 2018, Ch. 3.
- 9 D. Exerowa, D. Kashchiev, D. Platikanov. Stability and Permeability of Amphiphile Bilayers. *Adv. Colloid Interface Sci.* 40 (1992) 201-256.
- 10 G. Gochev, I. Retzlaff, D. Exerowa, R. Miller. Electrostatic stabilization of foam films from β -lactoglobulin solutions. *Colloid Surfaces A* 460 (2014) 272-279.
- 11 A. Javadi, N. Mucic, M. Karbaschi, J.Y. Won, M. Lotfi, A. Dan, V. Ulaganathan, G. Gochev, A.V. Makievski, V.I. Kovalchuk, N.M. Kovalchuk, J. Krägel, R. Miller. Characterization methods for liquid interfacial layers. *Eur. Phys. J. Spec. Top.* 222 (2013) 7-29.
- 12 V. Ulaganathan, I. Retzlaff, J. Won, G. Gochev, D. Gunes, C. Gehin-Delval, M. Leser, B. Noskov, R. Miller. β -Lactoglobulin adsorption layers at the water/air surface: 2. Dilational rheology: Effect of pH and ionic strength. *Colloids Surfaces A* 521 (2017) 167-176.